Journal Name

ARTICLE

Evaluation of the role of graphene-based Cu(I) catalysts in borylation reactions

Received 00th January 20xx,
Accepted 00th January 20xx

DOI: 10.1039/x0xx00000x

www.rsc.org/

Mario Franco,[a] Raquel Sainz,[b] Al Mokhtar Lamsabhi,[c,d] Cristina Diaz,[e] Mariola Tortosa[a,d] and M. Belén Cid*[a,d]

Carbon-supported catalysts have been considered as macromolecular ligands which modulate the activity of the metallic catalytic center. Understanding the properties and the factors that control the interactions between the metal and support allows a fine tuning of the catalyzed processes. Although huge effort has been devoted to comprehending binding energies and charge transfer for single atom noble metals, the interaction of graphenic surfaces with cheap and versatile Cu(I) salts has been scarcely studied. A methodical experimental and theoretical analysis of different carbon-based Cu(I) materials in the context of the development of an efficient, general, scalable, and sustainable borylation reaction of aliphatic and aromatic halides has been performed. We have also examined the effect of microwave (MW) radiation in the preparation of these type of materials using sustainable graphite nanoplatelets (GNP) as a support. A detailed analysis of all the possible species in solution revealed that the catalysis is mainly due to an interesting synergetic Cu_2O/graphene performance, which has been corroborated by an extensive theoretical study. We demonstrated through DFT calculations at a high level of theory that graphene enhances the reactivity of the metal in Cu_2O against the halide derivative favoring a radical departure from the halogen. Moreover, this material is able to stabilize radical intermediates providing unexpected pathways not observed using homogeneous Cu(I) catalysed reactions. Finally, we proved that other common carbon-based supports like carbon black, graphene oxide and reduced graphene oxide provided poorer results in the borylation process.

Introduction

Most heterocatalysts, which are crucial tools in the development of sustainable processes, involve metals or metallic salts anchored on an appropriate support.[1] It is well documented that the support is not merely a carrier of the catalyst that prevents aggregation but also it may actually contribute to its catalytic activity.[2] In this sense, graphene and graphene derivatives, due to their unique properties, are considered to be ideal two-dimensional supports to enhance the catalytic properties of metal nanoparticles (MNPs).[3,4] Two of the most outstanding features of graphene as a support are the available surface that favors adsorption of reagents, and the proposed overlapping between its π-orbitals and the d electrons of the transition metals that stabilize the MNPs, modulating their catalytic properties.

Although many metallic graphene-based materials have proven useful as catalysts in different processes,[3] the knowledge acquired is difficult to rationalize and, therefore, progress in the area is challenging. This is due to several reasons. There are a wide variety of graphene supports, whose structure changes according to the commercial source or the preparation method used. In addition, to support a given metal, different reagents and conditions have been applied, which directly affects the structure of the material. In this sense, it is worth mentioning some precedents that use microwave heating to fix metals on graphene derivatives, providing materials with high catalytic activity.[5–8] Furthermore, more effort has been devoted to developing synthetic applications rather than trying to understand the structure of the materials and the active catalytic species.[9] More profound studies which correlate structure/catalysis in carbon-supported catalysts have been done in single noble metal catalysts.[10] The important role of graphene as a support has been mainly studied when using Pd heterogeneous catalysts.[11] A deeper understanding of the interactions between graphene and different metallic nanoparticles (MNPs) and their consequences in terms of energy and electronic density would help to design supported catalysts that are accessible, sustainable and recyclable and, therefore, new and efficient catalytic processes.

Organoboron compounds are of noteworthy value in organic synthesis[12] as well as in medicinal chemistry.[13] Boronic esters, especially boronic acid pinacol esters (RBpin),[14] which are stable and easy to purify, can be easily transformed into a wide range of functional groups to provide access to a broad array of diverse molecules,[15] with the Suzuki–Miyaura coupling reaction being the most extensively applied.[16] Therefore, the development of sustainable methods to introduce the boronic ester moiety into organic compounds with high efficiency is a topic of great interest. In

---

[a] *Department of Organic Chemistry, Universidad Autónoma de Madrid, Cantoblanco, 28049 Madrid (Spain), E-mail: belen.cid@uam.es.*
[b] *Institute of Catalysis and Petrochemistry, CSIC, C/Marie Curie 2, 28049 Madrid (Spain).*
[c] *Department of Chemistry, Universidad Autónoma de Madrid, Cantoblanco, 28049 Madrid (Spain)*
[d] *Institute for Advanced Research in Chemical Sciences (IAdChem), Universidad Autónoma de Madrid, 28049 Madrid, Spain.*
[e] *Departamento de Química Física, Facultad de CC. Químicas, Universidad Complutense de Madrid, 28040 Madrid, Spain*

this sense, transition metal-mediated borylations[17] are key tools. Particularly useful are nucleophilic copper-boryl species due to the low cost of the metal catalyst, as well as the wide functional group tolerance and mild reaction conditions required.[18] This approach has been used to borylate aromatic[19] and aliphatic[20,21] halides in high yields.[22]

To overcome the drawbacks associated with homogeneous metallic catalysis such as the use of ligands, metal contamination of compounds and incapability of reusing the catalyst, the development of heterogenous catalysts and in particular of nanoparticles in borylation reactions has attracted some attention.[23,24] In 2014, Chung described the borylation of a variety of primary and secondary alkyl bromides using B_2pin_2 to give the corresponding alkyl boronates using commercially available copper nanoparticles (Cu NPs). Despite the relatively broad functional group tolerance, no reuse of the catalysts was reported.[25] One year later, in order to avoid nanoparticle aggregation and therefore to favor recyclability, Huang and Xu reported the laborious preparation of Cu_2ONPs/CB, Cu_2O nanoparticles (NPs) supported on carbon black (CB), and their use in the borylation of primary and secondary alkyl bromides. Nevertheless, after the third cycle, a decrease of efficiency due to nanoparticle aggregation prevents further recycling.[26] During the preparation of this manuscript, Bose described the borylation of alkyl halides using magnetically recoverable Cu(II) nanoparticles (Scheme 1).[27]

Aromatic halides have been borylated using copper ferrite nanoparticles, but no recyclability was reported.[28]

According to precedents,[29] the development of new materials able to borylate both aromatic and aliphatic halides under mild conditions with good recyclability properties would be an excellent scenario to improve the catalytic activity of this class of materials and progress in the knowledge of the effect of different graphenic supports in catalytic processes. We have recently published the preparation and some synthetic applications under continuous and flow conditions of a new material, graphenit-Cu(I) (A).[30] It is easy to prepare from cheap and sustainable nanoplatelets (GNPs) and, according to X-ray powder diffraction, contains Cu_2O in the matrix; it is also highly dispersible, effective as a catalyst, robust and reusable. As a continuation of our interest in taking advantage of the ability of graphene derivatives to modulate the catalytic activity of an anchored catalyst,[31,32] we have focused our efforts on the development of an efficient, ligand-free and sustainable general borylation protocol.[33–37] In the context of this reaction, we have performed a systematic study paying special attention to understanding the factors that affect the catalytic activity. For that, we have studied the catalytic species that could be present in solution as well as the effect of microwave radiation during the preparation of the material on the structure, catalytic activity and recyclability, analyzing the composition of the materials before and after catalysis. Moreover, we have performed DFT calculations at a high level of theory to analyze graphene and MNP interactions as well as substrate interactions. Finally, we have evaluated comparable materials using different supports but the same procedure of preparation.

Experimental

Preparation of material A

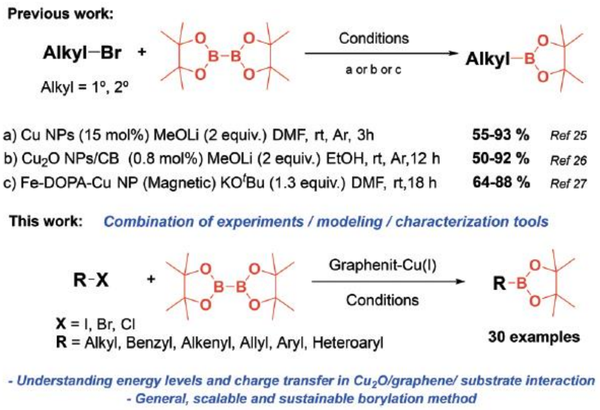

Scheme 1 Precedents and outline of the present heterogeneous reaction.

A suspension of graphenit-O_x (1.75 g) in deionized H_2O (175 mL) was sonicated for 1 h. Then, $CuCl_2$ (381 mg, 2.83 mmol) was added and the mixture was vigorously stirred at room temperature for 16 h. After that, the mixture was cooled down to 0 °C and a solution of $NaBH_4$ (227 mg, 6.00 mmol) in deionized H_2O (175 mL) was added dropwise over 30 min. After stirring at room temperature for 24 h, the material was filtered, washed with deionized water (4 Å~ 50 mL) and acetone (3 Å~ 50 mL), and finally dried under vacuum for 4 h to afford 1.98 g of graphenit-Cu(I).

Preparation of materials B–EMW

To a suspension of graphenit-Ox (500 mg) in deionized H_2O (100 mL), $CuCl_2$ (100 mg) was added, and the mixture was sonicated for 1 h. Then, $NaBH_4$ (65 mg) diluted in 25 mL of D.I. water was added dropwise to the suspension which was vigorously stirred at 0 °C. Once the addition of the reductant was complete, the flask was placed into a conventional microwave and was irradiated for the corresponding time (see Table 1) at 560 watts. After this time, the flask was stirred manually outside the microwave for 40 seconds and the process was repeated for the corresponding number of times (see Table 1). Once the microwave cycles were finished and the mixture reached r.t., the material was filtered and washed with D.I. water and acetone. Finally, the material was dried in a vacuum tube at 60 °C overnight.

General considerations for the borylation procedure

The indicated mixture of reagents and solvent specified in each case was sonicated for 5 minutes. Although some reactions were performed in a glovebox, we demonstrated that the reactions work under an Ar atmosphere using Schlenk techniques. In the case of aliphatic halides, the reaction also works without an Ar atmosphere in most of the cases. The copper amount added to each experiment was calculated based on the % wt Cu determined through TXRF for each material. After the corresponding times (see Tables 1–4), the catalyst was separated from the mixture by centrifugation at 7000 rpm, collecting the supernatant. Once separated, the catalyst was washed, resuspended in the indicated solvent, and separated by centrifugation, collecting the supernatant. This process was repeated

Table 1 Preparation of materials using microwave radiation and study in click and borylation reactions

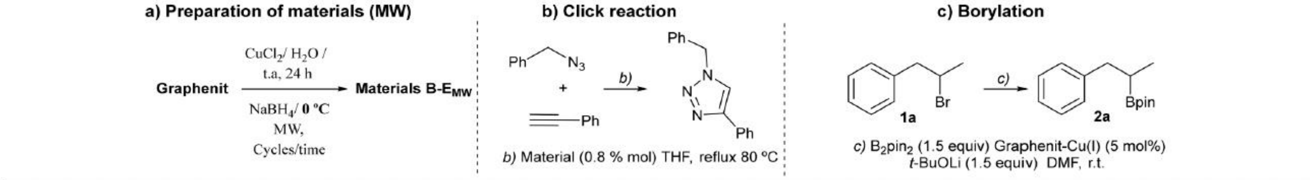

	MW^a cycles/t (s)		Crystallite size^c (nm)	Click reaction^d (conv)		Borylation^e (conv)	Cu (%)
Entry	Materials (A–E)	Cu^b (%)	Cu(I)/Cu(0)	(3 h)	(1 h)	30 m	After borylation/% loss^f
1	**A**	6.4	19/—	100	64	100	5.9/7.8
2	6/10 s (60 s) $\mathbf{B_{MW}}$	6.8	4/12	39	37	61	6.0/11.8
3	3/20 s (60 s) $\mathbf{C_{MW}}$	8.7	4/17	59	37	64	7.0/19.5
4	12/10 s (120 s) $\mathbf{D_{MW}}$	7.5	11/14	46	33	56	7.4/1.3
5	2/30 s (60 s) $\mathbf{E_{MW}}$	6.9	14/7	61	39	61	6.8/1.45

^{a} Number of cycles and time per cycle, total time in brackets. ^{b} Determined by total reflection X-ray fluorescence (TXRF). ^{c} Estimated from the peak width of the (111) Bragg reflection by using Scherrer's equation. ^{d} Conversion determined by ^{1}H NMR under conditions (b): benzyl azide (0.43 mmol), phenyl acetylene (1 equiv.), material (0.8% mol), THF, reflux 80 °C. ^{e} Conversion determined by ^{1}H-NMR under conditions (c): bromide (0.25 mmol), B_2pin_2 (1.5 equiv.), graphenit-Cu(I) (5 mol%), *t*-BuOLi (1.5 equiv.), DMF, r.t. ^{f} Percentage of Cu loss in recycled materials.

two more times. The collected organic phases were then washed with water. The combined organic phases were then dried over $MgSO_4$, filtered, and concentrated at reduced pressure. All borylated compounds were purified by column chromatography using deactivated silica gel (Et_3N 5% w/w) and a cyclohexane : ethyl acetate mixture as the eluent.

Borylation procedure for the alkyl halides (conditions A).

In a vial, the catalyst (5 mol%), bis(pinacolato)diboron (95 mg, 0.38 mmol/127 mg, 0.5 mmol, see Table 2) and t-BuOLi (30 mg, 0.38 mmol) were added to 1 mL of dry DMF, and the mixture was sonicated. Then the alkyl bromide (0.25 mmol) was added, and the mixture was stirred vigorously at room temperature. Et_2O was used to rinse out the catalyst and theorganic layers were washed 3 times to eliminate DMF.

Borylation procedure for the aryl iodides (conditions B).

In a screw-capped vial, the catalyst (2.5 mol%) was added and then placed into a glovebox. There, bis(pinacolato) diboron (159 mg, 0.63 mmol), t-BuOLi (30 mg, 0.38 mmol), the aryl iodide (0.25 mmol) and 1 mL of dry THF were added. Outside the glovebox, the vial with the mixture was then sonicated. The mixture was stirred vigorously at 60 °C for 24 h. After this time, the catalyst was washed and resuspended with EtOAc.

Borylation procedure for the aryl bromides (conditions C).

In a screw-capped vial, the catalyst (5 mol%) was added and then placed into a glovebox. There, bis(pinacolato)diboron (159 mg, 0.63 mmol), MeONa (20.5 mg, 0.38 mmol), the aryl bromide (0.25 mmol) and 1 mL of dry DMA were added. Outside the glovebox, the vial with the mixture was then sonicated. The mixture was stirred vigorously at 60 °C for 6 h. After this time, the catalyst was washed and resuspended with EtOAc.

Computational details

Density functional theory (DFT) calculations under periodic boundary conditions (PBC) have been carried out using the plane-wave based code VASP.[38–40] To describe the exchange–correlation energy of the electrons, we have worked within the generalized gradient approximation (GGA). In applying the GGA, we have used the PBE functional[41] corrected to take into account the van der Waals dispersion forces following the D3 correction proposed by Grimme[42] including Becke–Johnson damping.[43] The expansion of the single-particle Kohn–Sham Bloch states has been truncated for a kinetic energy higher than 550 eV. The projector-augmented method (PAW)[44] has been used to describe the core electrons. A convergence criterion of 1 Å~ 10−5 eV Å−3 for the Hellmann–Feynman forces has been used for all the geometry optimization calculations, which have been performed using a conjugated-gradient approach. Finally, the adsorbate/substrate system has been modelled using a (6 Å~ 6) unit cell. Taking into account the size of the unit cell, to sample the Brillouin zone only the gamma-point has been considered. On the other hand, estimating the energy profile of radical formation using the DFT-PBC approach requires huge computational resources; therefore, to perform such analysis with reasonable computational effort, we chose the ONIO method.[45] The election of the graphene sheet was conditioned by the size of reaction space. In line with our recent work[32] and following the same reasoning, a graphene sheet constituted by 9 Å~ 5 benzene rings divided in two layers seemed to be adequate to describe the chemical processes under study. The optimization for the high layer was achieved at B3LYP/6-31G(d,p)[46,47] while for the low layer the level of theory was B3LYP/3-21G. In order to include the van der Waals dispersion forces, the D3-correction proposed by Grimme[42] was applied. All the calculations were done using the Gaussian 16 series of programs.[48] The electronic population analysis was done by means of quantum theory of atoms in molecules (QTAIM)[49] using the AIMAll suite of programs.[50] A data set collection of computational results is available in *the ioChem-BD repository*.[51]

Results and Discussion

Table 2 Scope of borylation reactions of aliphatic halides

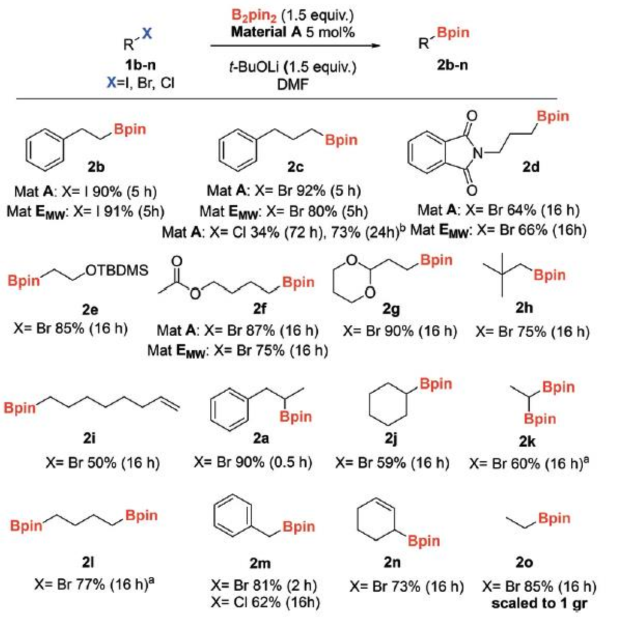

Conditions A: reactions were carried out at 25 °C using 5 mol% material **A**, 1 mL DMF, 0.38 mmol B_2pin_2, 0.38 mmol *t*-BuOLi, and 0.25 mmol alkyl bromide unless otherwise stated. Yields shown are those of purified, isolated products. [a] 0.5 mmol B_2pin_2. [b] TBAI (1 equiv.), 80 °C. For more detailed reaction conditions, see the ESI.†

Before performing our wide and deep systematic study, we needed to explore the catalytic activity of material A in the borylation reaction, our target transformation. For that purpose, we optimized the conditions using 1a as a secondary alkyl bromide model and bis(pinacolato)diboron as a boron source. Gratifyingly, the corresponding borylated product (2a) could be isolated in 90% yield using typical borylation conditions,20 t-BuOLi as a base, DMF as a solvent and 5 mol% of catalyst charge after 30 minutes at room temperature (Scheme 2).[52]

As mentioned above, it is known that the interaction between the metal and graphene surface can significantly affect the electron transfer properties of the metal and therefore its catalytic activity.[53] It has been demonstrated that graphenic materials of Pd and Pd–Ni prepared using microwave radiation display more strongly anchored metal nanoparticles and lower activation energy in several steps of Suzuki reactions.[53] This behavior has been explained on the basis of the formation of defects on the surface of graphene that favors interaction with the metal, allowing the support to act as both a charge donor and a charge acceptor favoring the different steps of the catalytic cycle. To the best of our knowledge, this effect has not been studied when using inexpensive copper salts in sustainable graphitic supports such as nanoplatelets.[54] Therefore, we decided to study the impact of MW radiation on Cu_2O/graphene based materials from several perspectives.

Our theoretical calculations based on DFT-PBC show that copper atoms of Cu_2O and the graphene layer exchange electronic density, and as a consequence, the molecules get adsorbed on the surface (see Fig. 1). As can be observed from the comparison between Fig. 1(b) and (d), the presence of a defect, in this case a single vacancy (SV), induces an increase of the electronic density exchanged, and this is reflected in the adsorption energy, that increases by an amount of 398 kJ mol^{-1} from pristine (a and b) to SV-graphene (c and d). Interestingly, these results do not depend on the number of graphene layers considered in the calculation.[52]

Therefore, expecting that MW radiation offers interesting metallic salt/support interactions and provides new heterogeneous graphene-based Cu-materials with applications in catalysis, we prepared and analysed a series of materials (Table 1). For the sake of clarity, all materials prepared following this method have been identified using MW as a subscript. Materials BMW–EMW were formed using different durations of MW radiation in different cycles (entries 2–5) following similar conditions to the ones used in the preparation of related materials. Their structure and catalytic activity were analysed in two different processes, click and borylation reactions. As can be seen in the left part of Table 1, in all the cases the content of copper (determined by TXRF) was around 7–8%, similar to graphenit-Cu(I) (A) prepared using an analogous method in the absence of microwaves (entry 1).[30] Interestingly, an increase of the total reaction time under microwave radiation to 120 s (entry 4) did not increase the ratio of copper (compare entries 2, 3, 5 and 4). According to X-ray powder diffraction data, material A prepared using Cu(II) and $NaBH_4$ in the absence of microwaves only evolves towards Cu(I) (entry 1), but the combination of both MW and NaBH4 afforded a mixture of Cu(I) and Cu(0) (entries 2–5).[52] When using the same conditions of preparation but just microwave heating (3 cycles of 20 s of microwave radiation) in the absence of $NaBH_4$, the material obtained contains only 0.3% of Cu.[52]

In order to compare the catalytic activity of material A and the new materials B_{MW}–E_{MW}, we used two model reactions. We tested the conversion in the click reaction between phenyl acetylene and benzylazide,[30,55] as well as in the borylation of the aliphatic compound 1a under the best optimized conditions. The click reactions were isolated after 3 h using 0.8 mol% of Cu. The materials obtained using MW radiation provided lower conversions than material A towards triazole formation (compare entries 1 and 2–5, middle part of Table 1). We hypothesized that this could be a consequence of the mixture of Cu(I) and Cu(0) species present,[52] so there is a smaller amount of active catalyst available for the reaction to occur since, as described in the literature, the reaction is catalysed by Cu(I). In the same way, all the materials obtained under microwave radiation (B–E_{MW}) were able to catalyze the borylation reaction but in a less efficient manner than material A. After 30 minutes, only around 60% conversion was obtained (entries 2–5, right part Table 1) but we observed that after 2 h, materials B_{MW}–E_{MW} provided full conversions. All the materials were recovered, and the amount of copper was analyzed after the borylation reactions by TXRF. Interestingly, although according to the TXRF data, a longer reaction time under microwave radiation (entry 4) does not increase the amount of copper, it fixes it in a more efficient way; after the reaction a smaller variation of copper contained in material D_{MW} than in the other ones (compare the last column of entries 1–5) is observed.

According to the results in Table 1, we decided to choose material E_{MW} as the optimal one prepared using MW radiation because it showed a good catalytic performance and suffers a very low percentage of leaching (entry 5).

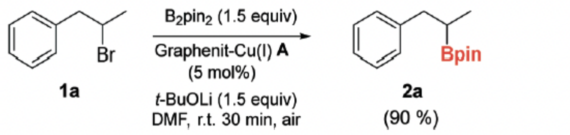

Scheme 2 Optimized conditions for the borylation reaction using graphenit Cu(I) A as a catalyst.

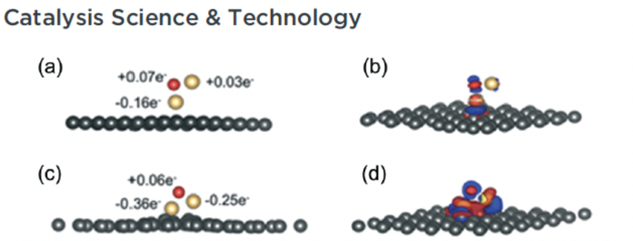

Fig. 1 Optimized structure and electronic density redistribution upon adsorption of Cu_2O on pristine graphene (a) and (b) and single-vacancy graphene (c) and (d). In (a) and (c), grey balls represent C atoms, red O and orange Cu. In (b) and (d), blue balls represent density accumulations and red density depletion. Isocontour value ±0.002 $e^- Å^{-3}$.

The next step was to examine the scope for a variety of alkyl halides in the borylation reaction (Table 2). As the analysis of Table 1 allowed us to identify graphenit-Cu(I) (A) as the optimal borylation catalyst for aliphatic halides, we performed this analysis using mainly material A. We demonstrated that the conditions were also applicable to primary substrates using iodides and bromides. It is noteworthy that even the more challenging chlorides56 also worked although in lower yields,[52] which could be improved when using TBAI.[25] We also proved that the reaction conditions were compatible with different functional groups such as phthalimides (2d), silyl ethers (2e), esters (2f), ketals (2g), and even terminal alkenes (2i) and bulky substrates (2h). For all of them the method afforded the desired borylated products with moderate to excellent yields.

The reaction was also extended to other secondary halides apart from the model substrate (2j), obtaining the corresponding borylated product with a similar yield. Moreover, by only adding an excess of the boron source, the diborylation of dibromoalkanes even the gem-substituted afforded the bis(boryl)alkanes (2k, 2l) easily. The reaction with activated halides such as benzylic (2m) and allylic (2n) substrates was also explored and deserve special comments, as it is known that they have the tendency to undergo homocoupling reactions.[20] After thorough optimization, we found that in the case of 2m, in the presence of toluene instead of DMF, the reaction turns selective to the formation of the homocoupled product.[52] Tertiary derivatives did not provide the corresponding borylated compounds.[57] Remarkably, under the same conditions, material EMW provided primary compounds 2b, 2c, 2d and 2f in similar yields. To demonstrate the possible application at the industrial level, we also prepared EtB(pin) (2o) in 85% yield starting from EtBr on a gram scale.

Next, we examined the catalytic activity of materials A and E_{MW} in the borylation of aromatic compounds. To our knowledge, there is no heterogeneous Cu-catalysts described able to promote the borylation of both aliphatic and aromatic halides (Table 3).[19,34]

We chose p-iodotoluene (3a) as a model substrate to test the borylation (Table 3). We observed some borylation ratio in the absence of a catalyst but in the presence of a base (22%).52 Unfortunately, under the optimized conditions used for alkyl halides, the borylated product 4a was obtained in low yield, with either catalyst A or E_{MW} (Table 3, entries 1 and 2). The low yield observed is mainly due to the formation of an undetermined amount of toluene (due to its volatility), which could be formed through a proto dehalogenation of 3a or proto deborylation of 4a. To understand the origin of the formation of toluene, we set up the reaction in the absence of B_2pin_2 and with 15 mol% of catalyst E_{MW} (entry 3). Under these conditions, a significant disappearance of aryl iodide 3a was observed. Additionally, when borylated product 4a was heated under the same reaction conditions, only a small percentage was lost (entry 4). These results suggest that the formation of toluene is due to the proto dehalogenation reaction of 3a under the reaction conditions. In the absence of a base, the reaction did not take place (entry 5). Reducing the catalyst loading to 2.5 mol% and the base amount to 1.5 equivalents, a better borylation/dehalogenation ratio was observed (compare entries 6 and 7). The use of THF (entry 8) instead of DMF significantly improved the yield. With these optimized conditions, catalyst A showed similar results (entry 9). Moreover, the reaction seems more sensitive to oxygen than to water (compare entries 10 and 11).[58] The borylation reaction of bromide 3b did not work under the reaction conditions optimized for the iodide 3a.[52] In this case, MeONa turned out to be a more efficient base and the reaction only worked when DMF or DMA was used as a solvent (entries 12–14).59 The chlorine derivative 3a' underwent a borylation reaction to some extent using material A and toluene as a solvent (entry 15).[52]

Since materials A and EMW provided similar results in borylation of aromatic halides, although EMW showed lower leaching of Cu than material A (Table 1), we decided to study the scope of the aromatic halides using mostly material E_{MW} (Table 4).

The optimized reaction conditions for iodides (entry 8, Table 3) and bromides (entry 14) could be applied to a variety of aromatic compounds with electron donating and withdrawing groups, to form the corresponding borylated products in moderate to good yields. Heteroaromatic halides like benzothiophenes (3k) and indols (3l) as well as olefinic substitution (3m) are also tolerated. Pyridines and benzofuranes did not work under the reaction conditions. The reaction of iodobenzene 4c was scaled up to 1 g of the starting material with no decline in the yield. No difference was observed when material A (graphenit-Cu(I)) was used to transform some chosen aryl halides (notes a, Table 4).

According to precedents, a radical mechanism would be expected.[20,22,26,60] The experiments performed with our catalytic system (Scheme 3) with the secondary and aromatic models pointed to the same direction; nevertheless, some subtle differences deserve some remarks. The presence of 2 equiv. of 2,2,6,6-tetramethylpiperidinyloxy (TEMPO) or butylated hydroxytoluene (BHT) completely inhibited the borylation reaction of 3a, which could suggest the presence of radical intermediates for the aromatic substrates (Scheme 3a).[61] In the same way, the reaction of the aliphatic bromide 1a did not provide 2a in the presence of BHT and TEMPO as a radical inhibitor and scavenger, respectively, but complex reaction mixtures (Scheme 3b). Moreover, a diastereomeric corresponding borylated product as a single diastereomer 2p, suggesting the formation of an alkyl flat intermediate and the entrance of the boron moiety through the less hindered face to form the more thermodynamically stable compound (Scheme 3c).

When we used the radical clock (bromomethyl)cyclopropane 1q as a substrate under the standard borylation reaction conditions, we did not observe the directly borylated product (2q), but a mixture of two different borylated products 5 and 6. The formation of the open product 5 in this reaction is quite well-known, indicating the presence of an alkyl radical intermediate.[21,26] However, the most surprising fact in this experiment is the presence of a cyclobutyl boronate (6) that, to the best of our knowledge, has not been observed in the borylation reaction of 1q before (Scheme 3d).[52]

The formation of product 6 (ref. 62) could suggest that the methyl cyclopropyl radical generated in the reaction could be stabilized by the graphene surface with enough time to evolve into

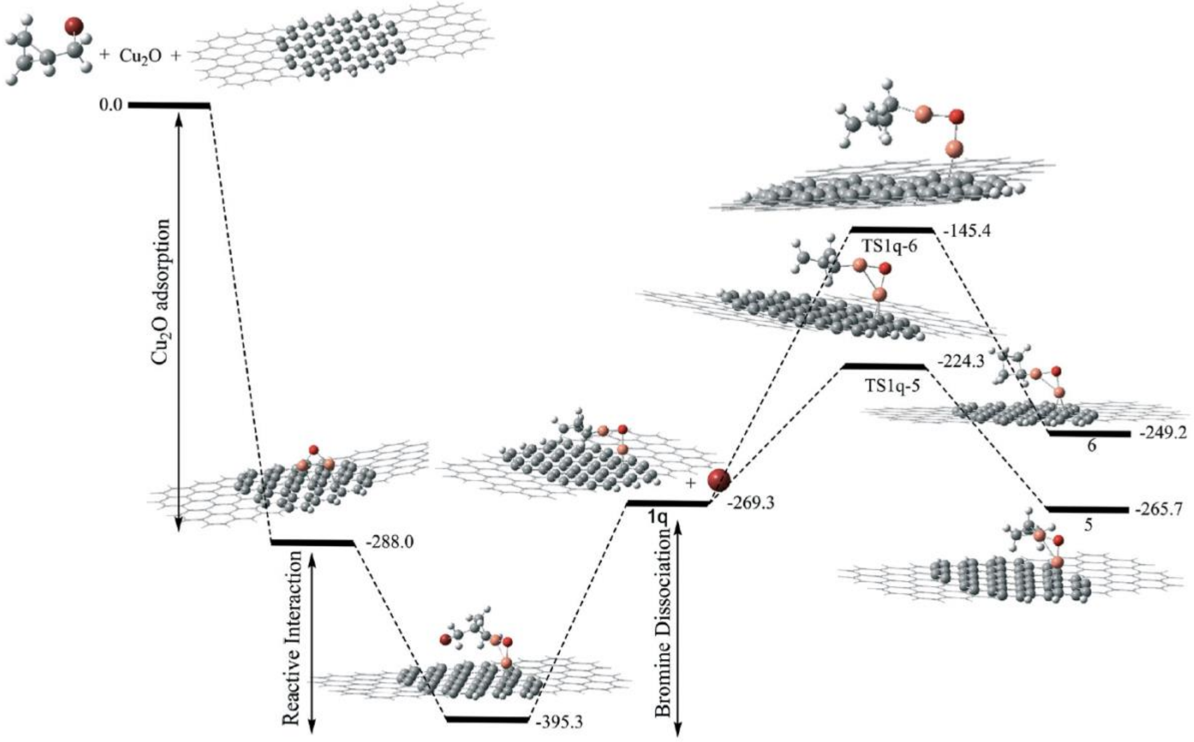

Fig. 2 Energy profile of the catalytic process of **1q** to attain **5** and **6** products (values are in kJ mol^{-1}), obtained by means of the ONIOM method.

Table 4 Scope of borylation reactions of aromatic halides

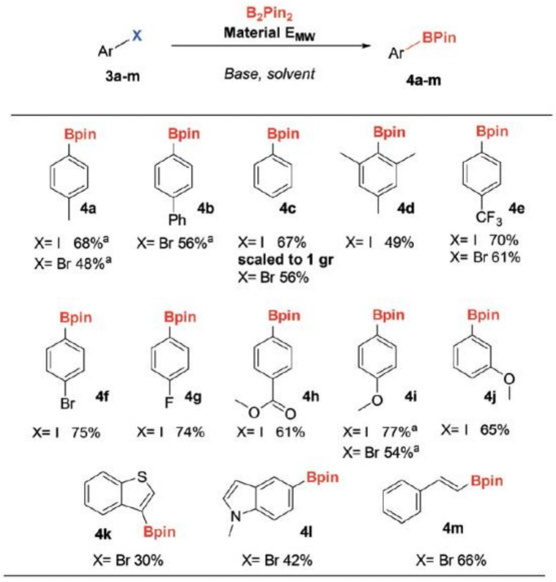

X = I (0.25 mmol), conditions B: B_2pin_2 (0.625 mmol, 2.5 equiv.), *t*-BuOLi (0.375 mmol, 1.5 equiv.), material $\mathbf{E_{MW}}$ (2.5 mol%), THF (1 mL), 60 °C, 24 h. X = Br (0.25 mmol), conditions C: B_2pin_2 (0.625 mmol, 2.5 equiv.), MeONa (0.375 mmol, 1.5 equiv.), material $\mathbf{E_{MW}}$ (5 mol%), DMA (1 mL), 60 °C, 6 h. ^{a} Reactions performed using material **A** gave the same results.

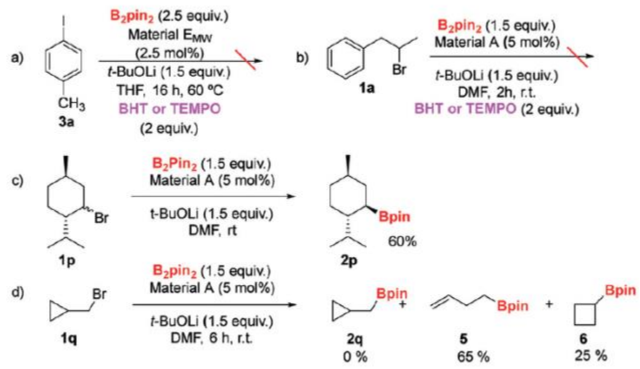

Scheme 3 Mechanistic study of the process.

mixture of the bromide derived from the menthol (1p) afforded the the cyclobutyl radical, which is borylated. We considered that a theoretical confirmation of this hypothesis would enhance the potential of this type of material which could be used in the future for non-viable transformations under conventional conditions. To confirm that, we explored the potential energy surface of the formation of both products 5. and 6. The objective was to estimate if the energy obtained from the interaction between graphene, Cu$_2$O and the reactant 1q would be sufficient to get the unexpected product 6. Effectively, the results of our calculations (based on the ONIOM method) as reported in Fig. 2 sustain such a hypothesis. In fact, the chemisorption of Cu$_2$O on graphene reports an energy gain of about −288 kJ mol^{-1}. If we add the interaction of 1q with this material (about 107 kJ mol^{-1}), the energy increases to about −395.3 kJ mol^{-1}. The radical dissociation of bromine is then ensured and so the evolution to the radical precursors of products 5 and 6, which occurs through transition states TS1q-5 and TS1q-6, respectively. The activation energy required for each product is in line with the yields observed experimentally. In fact, to get the most abundant product

(5) the reactant needs to surpass about 45 kJ mol^{-1}, whereas to reach product (6) the process requires about 124 kJ mol^{-1} as activation energy (see Fig. 2). It is worth noting that, at the same level of theory, we explored the energy profile for the formation of products 5 and 6 in the absence of graphene (see Fig. 3). The results pointed out that, after the bromine radical departure, the process to attain 5 is exothermic, in agreement with the experimental predictions. However, the mechanism to get product 6 is revealed to be endothermic, which disfavors the thermodynamic obtention of this compound experimentally. We should recall that the activation energy to attain 5 is much smaller than the energy barrier needed to reach 6. Comparing both pathways presented in Fig. 2 and 3, the importance of the adsorption of Cu_2O on graphene as a catalyst for borylation appears clear.

Once the generality and synthetic utility of the Cu-graphenit materials were demonstrated, we focused our attention on one of the main goals of heterogeneous catalysis, recyclability. We studied the yield of the borylation reaction of 1a with materials A and EMW after 2 hours of reaction. In all cases, the material was separated from the mixture by centrifugation, washed, dried under heat (60 °C) and vacuum, and reused in the next cycle. As can be seen in Table 5, although material EMW showed less leaching (Table 1), the yield dramatically drops in the 4th cycle (right column). When using material A the yield started to be lower In the 8th cycle (middle column).

To understand the different behavior of materials A and E_{MW}, we paid attention to the structure of both materials before and after they have been used (Ar, E_{MWr}). Table 6 collects the most relevant data regarding XPS, XRD and TEM.[52] TXRF data of each material are repeated for the sake of clarity in Table 6. The comparison of the composition observed by TXRF and XPS in each material gives a picture of the global amount of Cu and the Cu on the surface, respectively. Material A shows 6.4 wt% overall copper content (TXRF), much higher than the 1.2 wt% detected on the surface (XPS). This suggests that copper is mainly located in between the graphitic layers and not on the surface. Nevertheless, only 0.2 wt% is present on the surface of Ar (recovered after the reaction,) whereas 5.9% of the global copper is maintained, indicating that the loss of Cu after being used mainly occurs in the external layer. Materials E_{MW} and E_{MWr} showed a more constant composition of Cu, suggesting a more internal disposition and stronger interaction with the graphitic support.

There is also a clear difference in the oxidation state of Cu detected by XRD and by XPS on the surface. These techniques also give important information regarding the oxidation state of the metal for every material. In the case of materials A and Ar, only Cu_2O species are detected by XRD, whereas this technique detects Cu_2O and Cu(0) species for materials E_{MW} and E_{MWr}. Cu(II) is detected in all the cases but exclusively on the surface (using XPS). This result is reasonable due to the higher tendency to oxidation, due to the exposure to oxygen, of the external layer. Presumably, the small size of these particles prevents detection by XRD. The anchoring of the copper between internal layers would prevent oxidation and would explain the necessity for a previous treatment of the heterogeneous materials for exfoliation, using ultrasound, so that they are effective as catalysts.

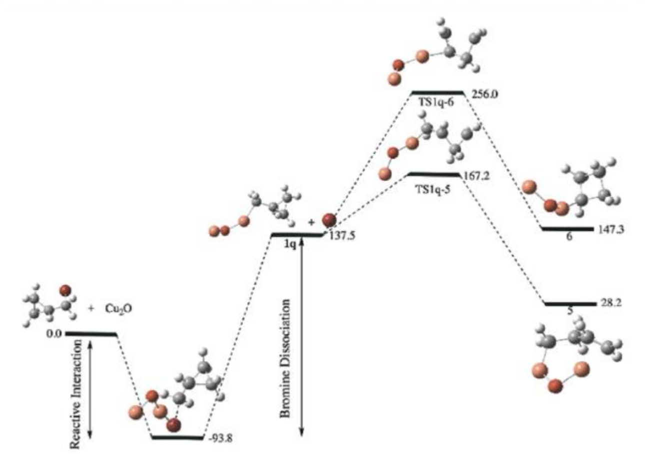

Fig. 3 Energy profile, at the B3LYP/6-311+G(d,p) level of theory, of the catalytic process of **1q** to attain the radical precursors of products **5** and **6** by complexation of Cu_2O (values are in kJ mol^{-1}).

The TEM images of A clearly show very well dispersed small particles (2 nm average diameter), which suffer some aggregation after catalysis in material Ar. In material EMW, the particles are not well dispersed but form aggregates, and the density of these aggregates, and the density of this aggregates increased with use. This fact, could be one of the reasons why E_{MW} presents lower activity and recyclability than material A. The TEM images of the E_{MWr} material allowed us to discard the hypothesis that the high content of Cu after recovery of material E_{MW}, prepared under MW radiation, could be due to the bigger average size of copper aggregates, which could have been recovered through centrifugation although they were not linked to the support, since no free copper particles are seen for the recycled materials.

Table 5 Recyclability in the borylation reaction of materials **A** and $\mathbf{E_{MW}}$

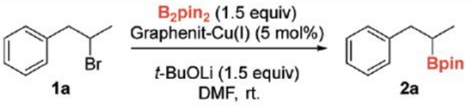

	Material **A**[a]	Material $\mathbf{E_{MW}}$[a]
Cycle	**2h** yield (%)	**2h** yield (%)
1	85	86
2	87	87
3	90	85
4	87	61
5	88	37
6	84	—
7	85	—
8	66	—

[a] Before the addition of the reagents, the mixture of the solvent and heterogenous material was kept for 5 minutes in an ultrasonic bath.

In order to get more insight into the catalytic species active in the reaction media and the role of the support, we carried out the model borylation reaction using different Cu species in the presence and in the absence of the support itself. According to the characterization data, material A contains Cu_2O almost exclusively. To unequivocally determine the role of the support and discard that any possible species in solution is responsible for the catalysis, we performed some control experiments using the secondary aliphatic model 1a (Table 7).

First, we discarded the existence of a background reaction as in the absence of a catalyst no compound 2a was detected (entry 2), compared with the 100% conversion obtained when using graphenit-Cu A (entry 1). We also determined that Cu_2O, graphenit or just the combination of both provides the starting material unaltered (entries 3–5). CuO was also unable to catalyze the reaction on its own or in the presence of graphenit (entries 6–7). According to the XPS and TXRF analysis, some traces of chlorides (0.03 wt%) are also present on the material. We reasoned that this could be due to the presence of the remaining $CuCl_2$, which is used as the copper source. Some CuCl could be formed as a result of the reduction in the treatment to form graphenit-Cu(I) (A). Therefore, to unambiguously discard that any of these species were responsible for the catalysis, we performed reactions of entries 8–11 using around 100-fold higher catalyst amount than the traces of chloride detected.[63] After 30 minutes, all the reactions showed lower conversions towards 2a than the reference reaction (entry 1). Although we cannot completely rule out a catalytic effect in this process due to these species, it should be insignificant. Interestingly, the presence of graphenit has a beneficial effect on the catalytic activity of $CuCl_2$ (entry 11).

Table 6 Most significant characterization data of materials **A**, **Ar**, $\mathbf{E_{MW}}$ and $\mathbf{E_{MWr}}$^{a}

Technique		Graphenit	Material **A**	Material $\mathbf{A_r}$	Material $\mathbf{E_{MW}}$	Material $\mathbf{E_{MWr}}$
TXRF	wt% Cu	—	6.4	5.9	6.9	6.8
XPS	HR regions wt%					
	C 1s O1s Cu 2p	C (98.6) O (1.4)	C (88.3) O (10.4) Cu (1.3)	C (93.2) O (6.6) Cu (0.2)	C (95.5) O (4.0) Cu (0.4)	C (96.1) O (3.6) Cu (0.3)
	Species of Cu (%) Cu(0) and Cu(I)/Cu(II)	—	15.6/84.4	28.9/71.1	21.0/79.0	29.0/71.0
XRD	Species of Cu	—	Cu(I)	Cu(I)	Cu(I) and Cu(0)	Cu(I) and Cu(0)
TEM		—	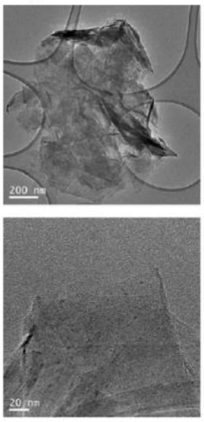	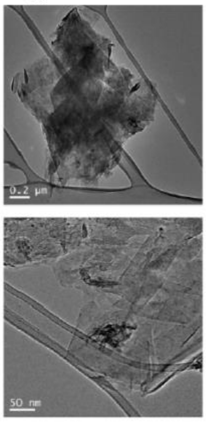	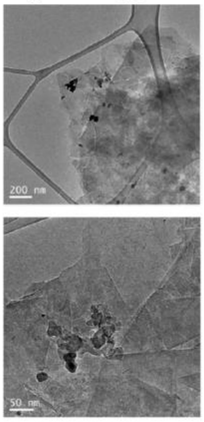	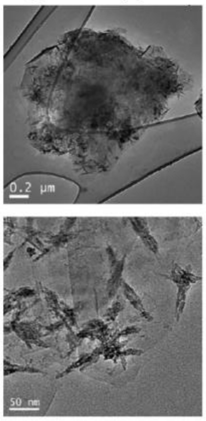

^{a} Subscript r refers to recycled materials after the borylation reaction.

Finally, we performed two control experiments to evaluate the role of the possible species in solution generated after ultrasound (US) treatment (entry 12) and/or the effect of the reagents (entry 13). For that purpose, we first maintained material A in a US bath for 5 minutes, centrifuged the solution and performed the reaction with the supernatant liquid which provided null conversion (entry 12). When material A was pretreated with US for 5 minutes, B_2pin_2 and t-BuOLi were added, the slurry stirred in DMF for 30 minutes at room temperature, and the material removed by centrifugation; the resulting supernatant solution was able to catalyze the transformation into 2a in 16% conversion after 30 minutes of the addition of 1 equiv. of 1a (entry 13). Therefore, only a low percentage of conversion could be attributed to the species in solution. Table 7 shows a remarkable catalytic performance of Cu_2O when it is properly anchored in material A. A similar behavior was observed with the aromatic halides (Table 8). In those cases, some background reaction is observed (compare entries 1 and 2). Cu_2O and graphenit have an insignificant catalytic effect on both halides (entries 3 and 4).

Null or very low conversions are observed when Cu_2O itself is used, in contrast with the analogous CuX (I, Br, Cl) which are excellent catalysts in borylation reactions.[20,21] Therefore, we decided to study theoretically the beneficial synergistic effect between the metal and support to disclose the changes exerted by the graphene surface in Cu_2O so that it is able to promote the borylation process. For this purpose, we analyzed the energy profiles and the electronic population of CuI and Cu_2O, free and anchored on graphene, in their interaction with alkyl halide 1q.

The comparison between the energy profiles involving Cu_2O supported on graphene (Fig. 2) and isolated copper oxide (Fig. 3) confirms the energy discrimination of the latter over the former. Furthermore, the analysis of the electronic density in the bond critical points (bcps) of the metal with halide 1q ratifies this discrepancy. In fact, the QTAIM population analysis of the complexes resulting from the interaction of Cu_2O, Cu_2O–graphene and CuI with (bromomethyl)cyclopropane (1q) highlights the differences in the electronic density estimated for the most important bcps (Fig. 4). The electrostatic binding of the metal in CuI and Cu_2O–graphene with 1q appears similar. It shows an electronic density of about 0.070 a.u. on its bcps. However, for free Cu_2O, the bcp depicted between the metal and cyclopropane presents a lower charge density (about 0.05 a. u). This means that the metal presents a weaker affinity to the halide in 1q when it is free than when it is supported on graphene. The role played by the support, acting indeed as a macromolecular ligand, is then crucial in the borylation process since it increases the interaction capability of the metal and so the catalytic efficiency of the whole material.

Finally, in order to get some more insights into the role of the support and rationalize the possible advantages and disadvantages for future applications, we systematically analyzed under the

Table 7 Control experiments performed with aliphatic secondary halide **1a**

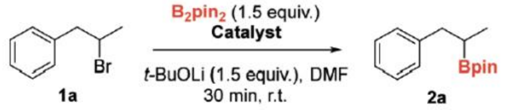

Entry	Catalyst	Conversion
1	Graphenit-Cu (**A**)	100
2	—	0
3	Cu_2O	0
4	Graphenit	0
5	Cu_2O + graphenit	0
6	CuO	0
7	CuO + graphenit	0
8	CuCl (2.9%)[a]	57
9	CuCl + graphenit [a]	51
10	$CuCl_2$ (3.5%)[a]	52
11	$CuCl_2$ + graphenit [a]	70
12	Supernatant US[b]	0
13	Supernatant US/B_2pin_2 *t*-BuOLi[c]	16

[a] Around 100-fold higher catalyst amount than the traces of chloride detected. [b] Supernatant liquid after 5 minutes of US treatment. [c] Supernatant liquid after 5 minutes of US treatment and stirring of a mixture of reagents for 30 minutes.

Table 8 Control experiments performed with aromatic halides

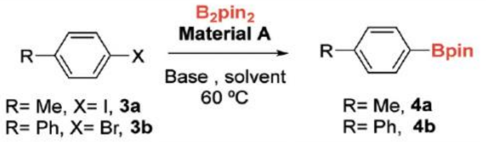

		3a	3b
		Conditions B[a]	*Conditions C*[a]
Entry	Catalyst	Conversion 6 h	Conversion 6 h
1	Graph-Cu (**A**)	28	100
2	—	2	6
3	Cu_2O	4	8
4	Graphenit	6	5

[a] X = I; *conditions B*: B_2pin2 (2.5 equiv.), *t*-BuOLi (1.5 equiv.), material **A** (2.5 mol%), THF (1 mL), 60 °C, 6 h. X = Br, *conditions C*: B_2pin_2 (2.5 equiv.), MeONa (1.5 equiv.), material **A** (5 mol%), DMA (1 mL), 60 °C, 6 h.

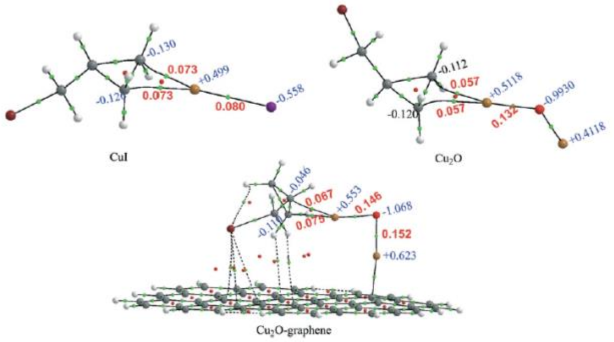

Fig. 4 Molecular graphs of the complexes of CuI, Cu_2O and Cu_2O–graphene with (bromomethyl)cyclopropane (**1q**). Green dots are the bond critical points and red dots are the ring critical points. The red values are the electronic density in a.u. and the blue values are the atomic charges.

optimized conditions in previous tables the borylation reactions for aliphatic bromides (conditions A) and aromatic iodides (conditions B) using comparable materials prepared from different traditional supports such as GO (F), rGO (G) or carbon black (H) but under the same conditions employed for material A (Table 9, entries 2–4).30 The behavior of the nanoparticles (I) generated using the same synthetic procedure used to prepare the previous materials without the corresponding support has also been studied (entry 5). To facilitate the comparison, results of material A and E_{MW} are also shown in Table 9 (entries 1 and 6).

When we focused on the borylation of the secondary aliphatic bromide 1a we analyzed conversions after 30 minutes, which clearly allowed us to determine the efficiency of every material.[64] Materials F (prepared from GO) and I (nanoparticles) afforded the poorest results (entries 2 and 5). Material G (prepared from rGO) afforded 80% conversion after 1 h of reaction. It is important to remark that rGO is obtained by reduction with hydrazine of GO, which in turn is prepared from graphite using Hummer's oxidation protocol that requires harsh conditions and hazardous reagents. Interestingly, material H which contains carbon black, a cheap and sustainable support, afforded comparable results (entry 4) to material A (entry 1). Nevertheless, a clear superiority of material A was observed when both materials (A and H) were analyzed in terms of stability and recyclability. That is to say, when using material H (7.2 wt% of copper) in the borylation reaction of 1a, the content of copper in the recovered material had decreased to 3.6 wt%, indicating an elevated leaching, probably due to a weak interaction between the metal and support.[52] In the case of the borylation of aromatic iodide 3a under conditions B, total conversions were observed for materials A, G, H and EWR after 24 h. Therefore, to determine unequivocally the efficiency of these materials, conversions were also determined after 8 h, with the materials prepared from nanoplatelets, materials A (entry 1) and EMW (entry 6) being the most effective. The fact that the simple unsupported nanoparticles NPs (I) are unable to catalyze the borylation of aliphatic halides reinforces the synergistic metal/graphene effect.

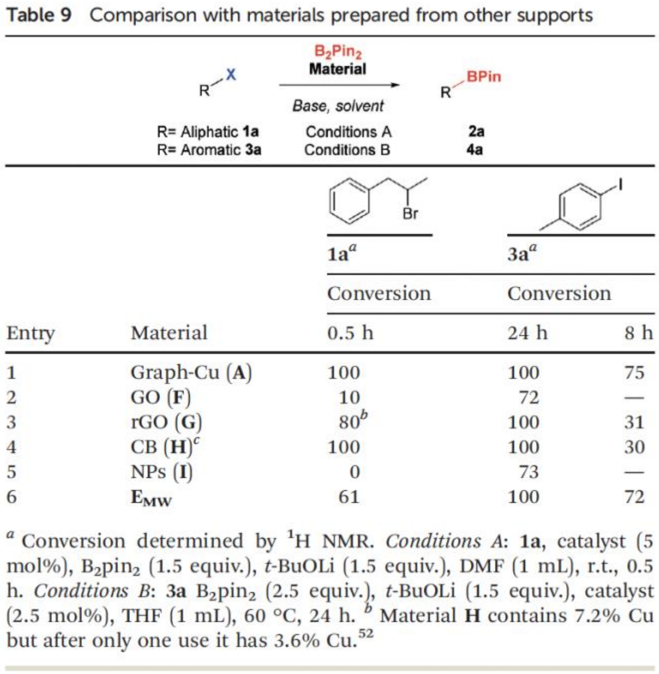

Table 9 Comparison with materials prepared from other supports

		1a[a]	**3a**[a]	
		Conversion	Conversion	
Entry	Material	0.5 h	24 h	8 h
1	Graph-Cu (**A**)	100	100	75
2	GO (**F**)	10	72	—
3	rGO (**G**)	80[b]	100	31
4	CB (**H**)[c]	100	100	30
5	NPs (**I**)	0	73	—
6	$\mathbf{E_{MW}}$	61	100	72

[a] Conversion determined by ^{1}H NMR. *Conditions A*: **1a**, catalyst (5 mol%), B_2pin_2 (1.5 equiv.), *t*-BuOLi (1.5 equiv.), DMF (1 mL), r.t., 0.5 h. *Conditions B*: **3a** B_2pin_2 (2.5 equiv.), *t*-BuOLi (1.5 equiv.), catalyst (2.5 mol%), THF (1 mL), 60 °C, 24 h. [b] Material **H** contains 7.2% Cu but after only one use it has 3.6% Cu.[52]

Conclusions

In conclusion, we have found that the Cu(I)-containing material A, prepared from cheap and sustainable nanoplatelets, is able to catalyze the borylation reaction of both aliphatic and aromatic halides in good to moderate yields. The material is not only a general and efficient catalyst, but it is also easily recyclable, and the reactions are scalable. The use of microwaves provided effective and strongly supported metallic materials but with lower generality and recyclability, presumably due to inactive Cu(0) and the formation of aggregates. Other classical graphenic supports provided poorer results in terms of efficiency and/or recyclability than material A. A detailed study of all the possible catalytic species revealed an interesting synergetic performance of Cu_2O when anchored to a graphenic support, which was corroborated by calculations at a high level of theory. The presence of graphene reinforces the electrostatic interaction between copper oxide and halide derivatives which enabled a radical departure of the halogen. The exploration of the potential energy surface of (bromomethyl)cyclopropane transformation with free and supported Cu_2O is a good example of the catalytic effect triggered by the presence of the graphene derivative. The surface promotes the electronic exchange between the species under study, stabilizing radical intermediates and favoring processes not described for typical Cu(I) homogeneous catalysis. This means that the metal presents a weaker affinity to the halide when it is free than when it is supported on graphene. Understanding the modulation of cheap, accessible, and sustainable salts such as Cu_2O by graphenic supports is valuable. Other transformations that are not viable under conventional conditions or require the presence of expensive noble metals and/or ligands are under study in our laboratory.

Conflicts of interest

There are no conflicts to declare.

Acknowledgements

We acknowledge the European Research Council (ERC- 337776) and the Spanish Government (CTQ2016-78779-R, PID2019-110091GB-I00, PID2019-107380GB-I00 and PDI2019-106732GB-I00) for financial support. We also thank Dr. Rafael Ferritto (Nanoinnova Technologies SL) for providing the graphenic materials and for the suggestion of the use MW radiation to anchor copper. A generous allocation of computing time at the Centro de Computación Científica of the UAM is also acknowledged.

Notes and references

[1] C. Descorme, P. Gallezot, C. Geantet and C. George, ChemCatChem, 2012, 4, 1897–1906.
[2] L. Lichen and A. Corma, Chem. Rev., 2018, 118, 4981–5079.
[3] For a review of metal nanoparticles supported on twodimensional graphene as heterogeneous catalysts see: S. Navalon, A. Dhakshinamoorthy, M. Álvaro and H. García, Coord. Chem. Rev., 2016, 312, 99–148.
[4] K. M. Yam, N. Guo, Z. Jiang, S. Li and C. Zhang, Catalysts, 2020, 10, 53–70 and references cited herein.
[5] H. M. A. Hassan, V. Abdelsayed, A. E. R. S. Khder, K. M. AbouZeid, J. Terner, M. S. El-Shall, S. I. Al-Resayes and A. A. El-Azharyb, J. Mater. Chem., 2009, 19, 3832–3837.
[6] A. R. Siamaki, A. E. R. S. Khder, V. Abdelsayed, M. S. El-Shall and B. F. Gupton, J. Catal., 2011, 279, 1–11. [7] Y. Yang, C. E. Castano, B. F. Gupton, A. C. Reber and S. N. Khanna, Nanoscale, 2016, 8, 19564–19572 and references cited herein.
[8] When using MW on GO as a support, it was demonstrated that it favors dispersion, minimizes aggregation, and removes oxygen content, reordering the basal plane carbon rendering the materials more similar to pristine graphene than when chemical reduction was used: D. Voiry, J. Yang, J. Kupferberg, R. Fullon, C. Lee, H. Y. Jeong, H. S. Shin and M. Chhowalla, Science, 2016, 353, 1413–1416.
[9] Y. Cheng, Y. Fan, Y. Pei and M. Qiao, Catal. Sci. Technol., 2015, 5, 3903–3916.
[10] C. G. Iann and P. Serp, Chem. Rev., 2020, 120, 1250–1349.
[11] See for example: Y. Yang, A. C. Reber, S. E. Gilliland, C. E. Castano, B. F. Gupton and S. N. Khanna, J. Catal., 2018, 360, 20–26 and references cited herein.
[12] Synthesis and Application of Organoboron Compounds, ed. E. Fernández and A. Whiting, Springer International Publishing, Cham, 2015.
[13] G. F. S. Fernandes, W. A. Denny and J. L. Dos Santos, Eur. J. Med. Chem., 2019, 179, 791–804.
[14] A. J. J. Lennox and G. C. Lloyd-Jones, Chem. Soc. Rev., 2014, 43, 412–443.
[15] T. Chinnusamy, K. Feeney, C. G. Watson, D. Leonori and V. K. Aggarwal, in Comprehensive Organic Synthesis, ed. G. A. Molander and P. Knochel, Elsevier, Oxford, 2nd edn, 2014, vol. 7, pp. 692–718.
[16] J. Magano and J. R. Dunetz, Chem. Rev., 2011, 111, 2177–2250.
[17] J. F. Hartwig, Chem. Soc. Rev., 2011, 40, 1992–2002.
[18] For a review of copper-boryl mediated reactions in organic synthesis see: D. Hemming, R. Fritzemeier, S. A. Westcott, W. L. Santos and P. G. Steel, Chem. Soc. Rev., 2018, 47, 7477.
[19] The first reported Cu-catalyzed borylation of aryl halides using B_2Pin_2: C. Kleeberg, L. Dang, Z. Lin and T. B. Marder, Angew. Chem., Int. Ed., 2009, 48, 5350–5354 (Angew. Chem., 2009, 121, 5454–5458).

[20] The first reported metal-catalyzed borylation of alkyl halides: P. G. Steel, T. B. Marder and L. J. Liu, Angew. Chem., Int. Ed., 2012, 51, 528–532 (Angew. Chem., 2012, 124, 543–547).

[21] H. Ito and K. Kubota, Org. Lett., 2012, 14, 890–893.

[22] For a general review about formal nucleophilic borylations see: K. Kubota, H. Iwamoto and H. Ito, Org. Biomol. Chem., 2017, 15, 285–300.

[23] For a review article about the nano-catalytic approach for C–B bond formation reactions see: P. K. Verma, M. L. Shegavi, S. K. Bose and K. Geetharani, Org. Biomol. Chem., 2018, 16, 857–873.

[24] For a review article about Cu and Cu-based nanoparticles in catalysis see: M. B. Gawande, A. Goswami, F.-X. Felpin, T. Asefa, X. Huang, R. Silva, X. Zou, R. Zboril and R. S. Varma, Chem. Rev., 2016, 116, 3722–3811.

[25] J. H. Kim and Y. K. Chung, RSC Adv., 2014, 4, 39755–39758.

[26] X.-F. Zhou, Y.-D. Wu, J.-J. Dai, Y.-J. Li, Y. Huang and H.-J. Xu, RSC Adv., 2015, 5, 46672–46676.

[27] M. L. Shegavi, A. Agarwal and S. K. Bose, Green Chem., 2020, 22, 2799–2803.

[28] B. Mohan, H. Kang and K. H. Parka, Catal. Commun., 2016, 85, 61–65.

[29] For a very recent report on the borylation reaction of alkyl bromides and chlorides catalyzed by graphene supported Cu/Pd alloy nanoparticles see: Z.-F. Jiao, Y.-M. Tian, X.-N. Guo, U. Radius, H. Braunschweig, T. B. Marder and X.-Y. Guo, J. Catal., 2021, 395, 258–265.

[30] S. De Angelis, A. Triminì, M. Franco, A. González, R. Sainz, L. Degennaro, G. Romanazzi, C. Carlucci, A. Goñi, V. Petrelli, R. Ferritto, J. L. Aceña, R. Luisi and M. B. Cid, Chem. – Asian J., 2019, 14, 3011–3018.

[31] E. Rodrigo, B. García Alcubilla, R. Sainz, J. L. García Fierro, R. Ferritto and M. B. Cid, Chem. Commun., 2014, 50, 6270–6273.

[32] R. Ramírez-Jiménez, M. Franco, E. Rodrigo, R. Sainz, R. Ferritto, A. M. Lamsabhi, J. L. Aceña and M. B. Cid, J. Mater. Chem. A, 2018, 6, 12637–12646.

[33] For our experience in transition-metal catalyzed borylations, see: R. Alfaro, A. Parra, J. Alemán, J. L. García Ruano and M. Tortosa, J. Am. Chem. Soc., 2012, 134, 15165.

[34] See also: L. Amenós, L. Trulli, L. Nóvoa, A. Parra and M. Tortosa, Angew. Chem., Int. Ed., 2019, 58, 3188.

[35] For a selected example of photoinduced C–B bond formations see: F. W. Friese and A. Studer, Angew. Chem., Int. Ed., 2019, 58, 9561–9564 (Angew. Chem., 2019, 131, 9661–9665).

[36] For alkyl and aryl iodides using blue light and DMF as a Lewis-basic solvent: Y. Cheng, C. Mück-Lichtenfeld and A. Studer, Angew. Chem., Int. Ed., 2018, 57, 16832–16836 (Angew. Chem., 2018, 130, 17074) and references cited herein.

[37] Advances in Organoboron Chemistry towards Organic Synthesis, ed. E. Fernández, Thieme, Stuttgart, Germany, 2020.

[38] G. Kresse and J. Hafner, Phys. Rev. B: Condens. Matter Mater. Phys., 1993, 47, 558–561.

[39] G. Kresse and J. Furthmüller, Phys. Rev. B: Condens. Matter Mater. Phys., 1996, 54, 11169–11186.

[40] G. Kresse and D. Joubert, Phys. Rev. B: Condens. Matter Mater. Phys., 1999, 59, 1758–1775.

[41] J. P. Perdew, K. Burke and M. Ernzerhof, Phys. Rev. Lett., 1996, 77, 3865–3868.

[42] S. Grimme, J. Antony, S. Ehrlich and H. Krieg, J. Chem. Phys., 2010, 132, 154104.

[43] S. Grimme, S. Ehrlich and L. Goerigk, J. Comput. Chem., 2011, 32, 1456–1465.

[44] P. E. Blöchl, Phys. Rev. B: Condens. Matter Mater. Phys., 1994, 50, 17953.

[45] S. Dapprich, I. Komáromi, K. S. Byun, K. Morokuma and M. J. Frisch, J. Mol. Struct.: THEOCHEM, 1999, 461–462, 1–21.

[46] C. Lee, W. Yang and R. G. Parr, Phys. Rev. B: Condens. Matter Mater. Phys., 1988, 37, 785–789.

[47] A. D. Becke, J. Chem. Phys., 1993, 98, 5648–5652.

[48] J. M. Frisch, et al., Gaussian 16, Revision C01, Gaussian,Inc., Wallingford CT, 2019.

[49] (a) R. F. W. Bader, Atoms in Molecules: A Quantum Theory, Clarendon Press Oxford Univ., Oxford, 1990; (b) C. F. Matta and R. J. Boyd, The Quantum Theory of Atoms in Molecules, Wiley-VCH Verlag GmbH & Co., KGaA, Weinheim, 2007.

[50] T. A. Keith, AIMAll (Version 19.10.12), TK Gristmill Software, Overland Park KS, USA, 2019, http://aim.tkgristmill.com.

[51] M. Álvarez-Moreno, C. de Graaf, N. Lopez, F. Maseras, J. M. Poblet and C. Bo, J. Chem. Inf. Model., 2015, 55, 95–103, DOI: 10.19061/iochem-bd-8-9.

[52] See the ESI† for more information.

[53] Y. Yang, A. C. Reber, S. E. Gilliland III, C. E. Castano, B. F. Gupton and S. N. Khanna, J. Phys. Chem. C, 2018, 122, 25396–25403.

[54] For microwave-assisted preparation of graphene-supported single atomicmetals: H. Fei, J. Dong, C.Wan, Z. Zhao, X. Xu, Z. Lin, Y.Wang, H. Liu, K. Zang, J. Luo, S. Zhao, W. Hu,W. Yan, I. Shakir, Y. Huang and X. Duan, Adv. Mater., 2018, 30, 1802146.

[55] Benzylazide was previously purified by flash chromatography.

[56] Higher temperatures (60 °C) and the addition of $(Bu_4N)I$ are required for this reaction to work when using CuI and PPh3 as a ligand (ref. 20). The use of bidentate Xantphos as a ligand is necessary to promote the borylation of secondary chlorides (ref. 21).

[57] Tertiary halides, including chlorides, undergo borylation using an NHC Cu(II) complex in: T. B. Marder, G. Bringmann, J. Maier, M. Haehnel, H. O. Omoregie, S. Brand and S. K. Bose, ACS Catal., 2016, 6, 8332.

[58] This behaviour has also been observed by Marder (see ref. 19) in the case of homogenous copper-catalysed reactions and it was rationalized by proposing a radical mechanism in which THF acts as a H radical donor.

[59] These solvents have demonstrated a key role in some borylation processes: A. Fawcett, J. Pradeilles, Y. Wang, T. Mutsuga, E. L. Myers and V. K. Aggarwal, Science, 2017, 357, 283–286.

[60] Q. Liu, J. Hong, B. Sun, G. Bai, F. Li, G. Liu, Y. Yang and F. Mo, Org. Lett., 2019, 21, 6597–6602.

[61] F. W. Friese and A. Studer, Chem. Sci., 2019, 10, 8503–8518.

[62] The preparation of this compound has been described by borylation of cyclobutyl bromide in ref. 26.

[63] The excess of $CuCl_2$ and CuCl was used to avoid errors in the weight of the catalysts.

[64] We could observe that after 2 h all the materials except F (GO as support) and I (Cu_2O NP) showed complete conversions.